



**HAL**  
open science

## ASTEC V2.2 code validation: Illustrative results and main outcomes

Patrick Chatelard, Laurent Laborde

► **To cite this version:**

Patrick Chatelard, Laurent Laborde. ASTEC V2.2 code validation: Illustrative results and main outcomes. Nuclear Engineering and Design, 2023, 413, pp.112547. 10.1016/j.nucengdes.2023.112547 . irsn-04195835

**HAL Id: irsn-04195835**

**<https://irsn.hal.science/irsn-04195835>**

Submitted on 8 Sep 2023

**HAL** is a multi-disciplinary open access archive for the deposit and dissemination of scientific research documents, whether they are published or not. The documents may come from teaching and research institutions in France or abroad, or from public or private research centers.

L'archive ouverte pluridisciplinaire **HAL**, est destinée au dépôt et à la diffusion de documents scientifiques de niveau recherche, publiés ou non, émanant des établissements d'enseignement et de recherche français ou étrangers, des laboratoires publics ou privés.



Distributed under a Creative Commons Attribution - NonCommercial - NoDerivatives 4.0 International License

# ASTEC V2.2 CODE VALIDATION : ILLUSTRATIVE RESULTS AND MAIN OUTCOMES

**Patrick Chatelard and Laurent Laborde**

Institut de Radioprotection et de Sûreté Nucléaire  
IRSN/PSN-RES/SAM, Saint Paul lez Durance cedex 13115, France  
[patrick.chatelard@irsn.fr](mailto:patrick.chatelard@irsn.fr), [laurent.laborde@irsn.fr](mailto:laurent.laborde@irsn.fr)

## ABSTRACT

Significant efforts are being continuously put for many years into the assessment of the severe accident integral code ASTEC developed by IRSN, through comparison with the results of most of the experiments developed internationally or through benchmarks with other severe accident simulation codes. For this assessment process, the IRSN code developers are supported by international partners, notably in the frame of the recent SNETP-NUGENIA ASCOM collaborative project.

This paper relates to the 3<sup>rd</sup> major version of the ASTEC V2 series, V2.2, that was released in 2021 to the ASTEC community. It aims at providing an overview of the ASTEC V2.2 validation by comparison to experimental data. After a reminder of the ASTEC validation strategy, the ASTEC V2.2 validation matrix is depicted, including more than 300 experimental tests conducted at various scales in more than 50 different facilities worldwide. Then some V2.2 results are discussed for a few representative applications. These calculation examples are selected in a way to cover diverse aspects of severe accident phenomenology in order to provide a good picture of the ASTEC V2.2 modelling status for both in-vessel and ex-vessel processes. Finally, the main lessons drawn from this quite large validation task are summarized, along with an evaluation of the current physical modelling relevance and how it relates to the current state-of-the-art. Based on those outcomes, the ASTEC V2.2 validity domain is specified and some prospects for further improvements are put forward.

## KEYWORDS

ASTEC, severe accident simulation code, validation

## 1. INTRODUCTION

The severe accident (SA) integral code ASTEC [1], developed by the French Institut de Radioprotection et de Sûreté Nucléaire (IRSN), aims at simulating an entire SA sequence in a nuclear water-cooled reactor from the initiating event up to the release of radioactive elements out of the containment. The 3<sup>rd</sup> major version of the ASTEC V2 series, V2.2 [2], was released in 2021 to the ASTEC community. With respect to former V2.1 [3], main improvements are not only on the physical models and the code capabilities, but also on the resolution of physico-numerical issues to improve the robustness and reduce the sensitivity to “cliff-edge” effects. In particular, one may quote: the updated Reactor Coolant System (RCS) thermal-hydraulics 6 equations scheme along with a special attention paid to shut-down state conditions [4, 5]; new recommendations for the core degradation modelling, including debris and corium description with solidus and liquidus temperatures for UO<sub>2</sub> and ZrO<sub>2</sub> close to values from post-mortem examinations of degradation tests (in previous versions, one had to define strongly lowered solidus and liquidus temperatures to reproduce the degradation); some new core degradation models (in particular specific radiative heat transfer models for intact and degraded cores) to better cope with BWR or SFP sub-channels configurations; a consolidated reflooding model for intact or damaged cores; new or improved models addressing the corium behavior in the lower plenum and In-Vessel melt Retention (IVR) related issues [6]; an extension of the

kinetics data for the gaseous phase chemistry model in the RCS through an account in the modelling for more fuel and control rod elements (key-issue to evaluate the iodine gas/aerosol partition entering the containment); several new models of the iodine behavior in the containment (radiolytic decomposition of metallic iodide aerosols, decomposition of iodine oxides...).

As to the validation of physical models, significant efforts are being continuously put from many years into the assessment of the ASTEC code through the validation using the data of most of the experiments developed internationally or through benchmarks with other SA simulation codes. For this assessment process, the IRSN code developers are supported by international partners, notably in the frame of the recent NUGENIA ASCOM collaborative project [7] carried-out under the aegis of the Sustainable Nuclear Energy Technology Platform (SNETP) association. In continuity to former validation tasks [8] [9] [10] [11], the ASTEC V2.2 assessment has been carried out against a wide experimental database covering the main SA physical phenomena while following up in parallel the full scale code-to-code benchmark activity on various transients for different types of Light Water Reactors (LWRs).

The present paper is however exclusively focused on the validation vs. experiments, meaning that the ASTEC assessment by means of benchmarks with other SA codes on reactor SA sequences is not tackled in this article. To find out more about those benchmark studies, one can refer for instance to [12] [13] [14] [15] [16] that provide good illustrations of such kind of comparative plant applications.

This paper recalls firstly the general approach for ASTEC V2 validation before displaying the composition of the ASTEC V2.2 validation matrix. ASTEC V2.2 validation results are then illustrated and discussed for several representative applications. These calculation examples are selected in a way to cover diverse aspects of SA phenomenology, i.e. to cover both in-vessel and ex-vessel processes in order to provide a good picture of the ASTEC V2.2 modelling status. Finally, the main lessons drawn from this comprehensive validation approach are summarized, along with an evaluation of the current physical modelling relevance and how it relates to the current state-of-the-art. Based on those outcomes, the ASTEC V2.2 validity domain is specified and some prospects for further improvements are put forward.

## **2. VALIDATION STRATEGY FOR THE ASTEC V2 SERIES**

ASTEC V2.2 evidently benefits from the intensive validation of former V2.1, V2.1.1 and V2.2b versions that was carried out between 2015 and 2020 not only by IRSN but also by foreign partners in the frame of the successive FP7 CESAM [9] [10] and SNETP-NUGENIA ASCOM projects (e.g. [17] [18] [19] [20] [21] [22] [23] [24]). In practice, most of the experiments that were analyzed few years ago with V2.1 have been again recalculated with V2.2 knowing that, thanks to an adequate instrumentation of the ASTEC input decks associated to dedicated regression tests, the V2.2 results have been then automatically compared with the V2.1 former results, thus allowing to identify any differences between the two ASTEC versions and relate them to the code evolution. Besides, the ASTEC V2.2 validation is of course supported by its own large set of French and international experiments that cover most aspects of SA phenomenology. Hence, the ASTEC V2 validation matrix is progressively enlarged to continuously account for the last decade newly available experiments in the field of SA.

The actual V2.2 validation matrix includes three different types of experiments: 1) Separate-Effect tests (SETs) that address a single phenomenon, often in small-scale facilities; 2) Coupled-Effect Tests (CETs) that address a few phenomena, in facilities typically of small to intermediate scale; 3) integral applications that allow checking the correct reproduction of coupling phenomena and the completeness of the modeling with respect to significant phenomena. For the latter, one may notably mention the four integral experiments of the Phébus FP program that coupled all the ASTEC modules involved for the primary circuit and the core, and for the containment. Analyses of the results obtained on the calculation of the TMI-2 and Fukushima-Daiichi accidents can also be included in this third category of code assessment activities.

Overall, the ASTEC V2.2 validation matrix comprises more than 300 experimental tests conducted at various scales in more than 50 different in-pile and out-of-pile facilities worldwide, using simulating or real materials. The detailed contents of the ASTEC V2.2 validation matrix will be provided later in the paper, over successive sub-sections dealing one by one with each SA key-phenomenon.

### 3. OVERVIEW OF THE ASTEC V2.2 VALIDATION

This section aims to provide a comprehensive picture of the ASTEC V2.2 validation achievements. So, this chapter is itself sub-divided into separate sub-sections, each one being focused on a SA key physical phenomenon. In each case, one or a few code-to-data comparison results are summarized for experiments that are selected so as to be representative of the ASTEC V2.2 whole validation process. Without any particular mention, results discussed in the following sections have been obtained with revision V2.2.0.

#### 3.1. Thermal-Hydraulics in the Reactor Cooling System (RCS)

In ASTEC, CESAR is the module dealing with the two-phase thermal-hydraulics in the primary (including the vessel) and secondary circuits. The validation matrix that was considered to evaluate the physical relevance of the CESAR models implemented in ASTEC V2.2 to cope with RCS phenomena covers both DBA basic phenomena (see Table 1) and, to some extent, SA conditions (see Table 2).

**Table 1. Main circuit thermal-hydraulics experiments used for ASTEC V2.2 validation**

Domain	Physical phenomena	Facility/ Program	Experiments
<b>RCS thermal-hydraulics</b>	Two-phase flow, heat transfers, wall friction, interface friction, phase separation, condensation...	Moby Dick, Patricia GV, Cosi, Coturne	Numerous SETs
	Complete T/H behavior in the RCS	BETHSY	tests #9.1b ( <i>ISP-27</i> ), #5.2e, #6.4, #6.9f, #6.9g

To illustrate such CESAR validation tasks, the simulation of an integral experiment that was operated by CEA in the BETHSY facility representing a scaled down three-loop model of a 900 MWe Framatome PWR [25] is proposed. The BETHSY 9.1b test, which was selected as ISP-27, consisted in a 2" cold leg break with unavailability of the high pressure security injection and with a delayed ultimate procedure. The break was located in the loop to which the pressurizer belonged. The BETHSY 9.1b overall system behavior is well predicted by ASTEC V2.2, as illustrated below for the evolution of the primary and secondary pressures (Fig. 1a), the primary and secondary mass inventories (Fig. 1b) and the maximum cladding temperature in the core (Fig. 1c).

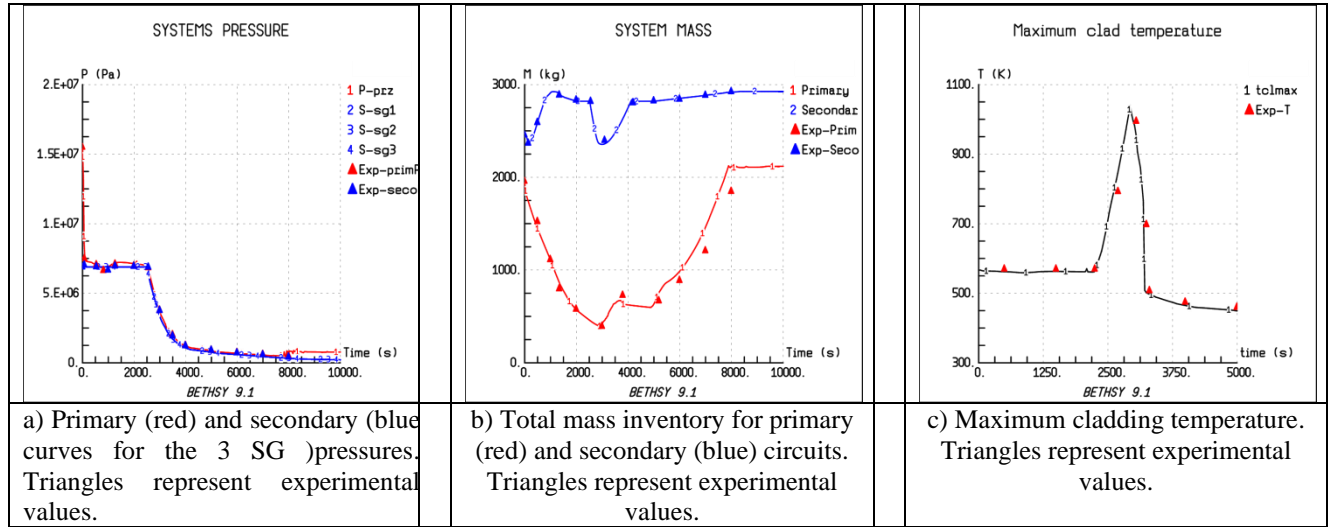


Figure 1. BETHSY 9.1b

Furthermore, as concerns the other BETHSY tests that have been considered to assess the ASTEC V2.2 thermal-hydraulics models, it is worth highlighting here that two of them have been especially retained to address shut-down state conditions, namely the tests 6.9f and 6.9g [4].

A summary of the main lessons that have been drawn from the code-to-data assessment in the field of RCS thermal-hydraulics is provided in the Section 4 of this paper. Details about these numerous and various ASTEC V2.2 CESAR simulations, may be found in [26] [27] [28] [29].

### 3.2. Core Degradation

In ASTEC, all in-vessel degradation processes (i.e. in the core region and in the vessel lower head) are simulated by the ICARE module. The validation matrix that was considered to evaluate the suitability and capability of the ASTEC V2.2 ICARE core degradation models is supplied in Table 2, knowing that these validation tasks necessarily require performing CESAR/ICARE coupled calculations.

Table 2. Main core degradation experiments (or accidents) used for ASTEC V2.2 validation

Domain	Physical phenomena	Facility/ Program	Experiments
Oxidation phenomena	Boron carbide oxidation	VERDI	16 tests
	Zry oxidation in air atmosphere	MOZART	7 tests
	Oxidation of U-O-Zr mixtures	SKODA UJP	18 tests
Core reflooding	Quenching of a fuel-rod assembly	PERICLES	48 tests
	Reflooding of a debris bed	PRELUDE	12 tests
		PEARL	33 tests
		DEBRIS	5 tests (bottom flooding) 2 tests (top flooding)
Core degradation	Early degradation phase in a PWR rod-bundle with quenching	QUENCH	Q-03, Q-06 ( <i>ISP-45</i> ), Q-08, Q-11,
	Early degradation phase in a VVER rod-bundle with quenching	QUENCH	Q-12
	Early degradation phase in a BWR core with quenching	QUENCH	Q-20

	Early degradation phase in a PWR rod-bundle exposed to air with final quenching	QUENCH	Q-10, Q-16
	Early and late degradation phases in a PWR rod-bundle	Phébus FP	FPT1 ( <i>ISP-46</i> ), FPT2, FPT3
		QUENCH	Q17
		PBF	SFD-1.4
	Debris bed and molten pool behavior	Phébus FP	FPT4
<b>Real severe accident</b>	RCS thermal-hydraulics and in-vessel degradation in a PWR	TMI-2 accident	phases 1 to 4
	BWR thermal-hydraulics and core degradation	Fukushima accidents	Fu-1, Fu-2, Fu-3

To illustrate such validation tasks, attention is directed hereafter at the works that were performed to assess the CESAR/ICARE coupled modules vs. the in-pile Phébus FPT1 and out-of-pile QUENCH-11 rod-bundle tests, and vs. the PEARL debris bed reflooding tests, respectively.

The Phébus FPT1 test aimed to investigate the fuel rod degradation in a PWR rod-bundle configuration, and the behavior of fission products released via the primary coolant circuit into the containment building. FPT1, which was selected as ISP-46, was the first test performed in the PHEBUS FP facility with irradiated fuel. The main objective was to obtain a significant degradation of the fuel rods to maximize the fission product releases. As to the transient sequence, the FPT1 experiment was sub-divided into a series of successive bundle power plateaus and power ramps according to the test protocol target temperatures [30].

The comparison between the ASTEC prediction and the experimental data looks good enough, as illustrated below for the temperature evolution of the fuel rods at different axial elevations (Fig. 2a), the total hydrogen production (Fig. 2b) and the final mass distribution along the test section (Fig. 2c). However, the total amount of relocated materials (debris + molten mixtures) is still a bit overestimated at the end of the test.

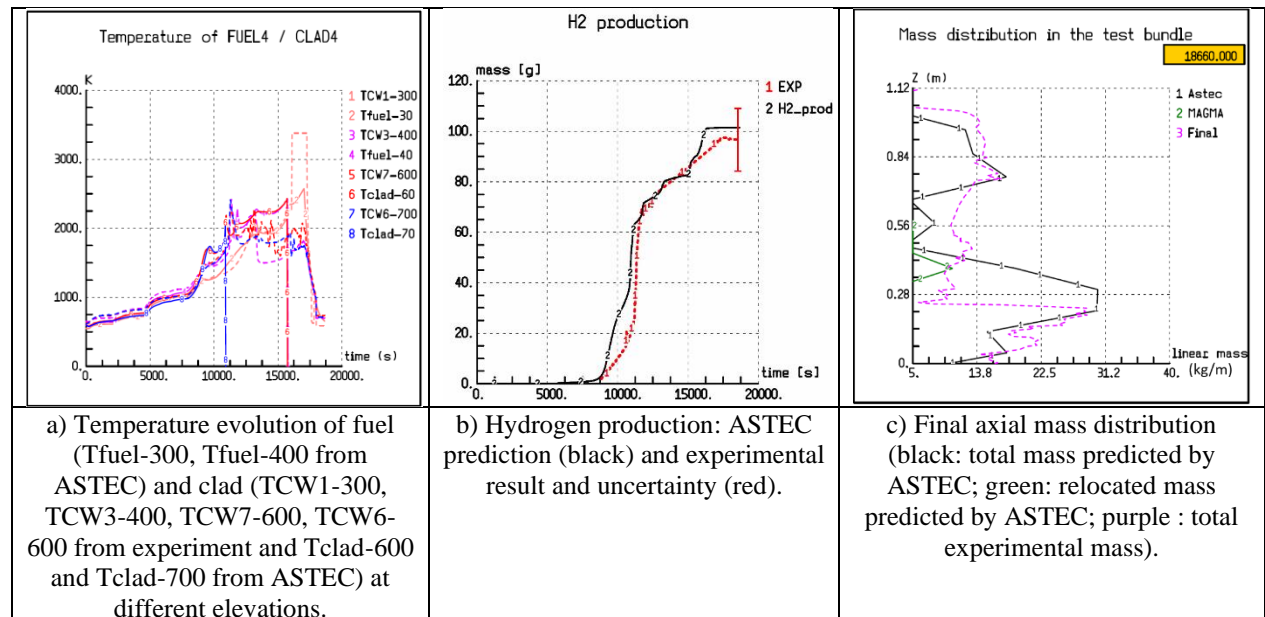


**Figure 2. Phébus FPT1**

The QUENCH-11 test aimed to investigate fuel rod degradation in a PWR rod-bundle configuration with a final quenching [31]. Unlike other QUENCH tests that started in a gaseous atmosphere, QUENCH-11 was

initiated with a test section full of water. The transient consisted of four phases: stabilization phase in water, boil-off phase with core uncover, heat-up phase and final bundle reflooding by bottom-up water quenching. The ASTEC V2.2 simulation of the QUENCH-11 test gives rather satisfactory results, as illustrated below for the temperature profiles (Fig. 3a and Fig. 3b, respectively during the heat-up phase and just before bundle quenching) and the total hydrogen production (Fig. 3c). Heat-up phases and temperature escalations are indeed rather well predicted, as well as the final quenching of the rod-bundle that is also simulated in overall agreement with the experimental data.

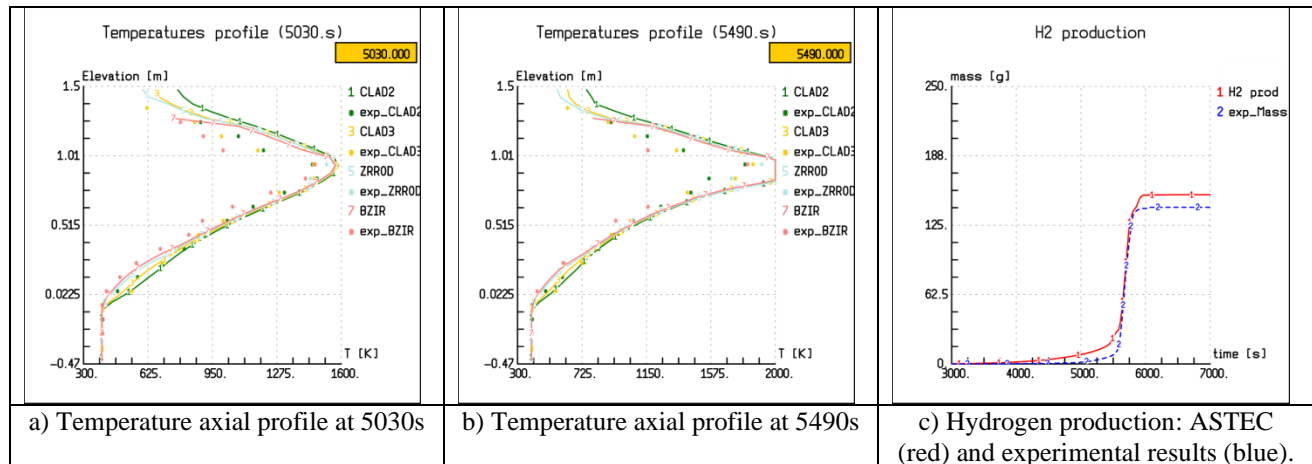


**Figure 3. QUENCH-11.** In profiles a) and c), stars represent experimental values. CLAD2 and CLAD3 are heat rods, ZRR0D is a corner non-heat rod, and BZIR represents the Zr shroud around the bundle

The ASTEC V2.2 validation vs. QUENCH data was performed within the frame of various projects. In particular, in connection to the ASCOM project, the analyses of the Q-08, Q-12 and Q-20 tests were performed by KIT [17] [18] [19] while ENEA focused on Q-06 in the frame of an IAEA uncertainty exercise [20].

Turning now to the late phase issues, the IRSN PEARL facility, which is part of the PROGRES experimental program [32], aims at improving the understanding of the factors governing the coolability of large, heated debris beds.

The PEARL test section (Fig. 4a) is composed of a long quartz tube (diameter 540 mm) filled with a 500 mm high debris bed made of stainless-steel balls. It is surrounded by a bypass zone made of twice larger quartz balls representing a quasi-intact region at the periphery of a degraded core. The bed is heated by induction with a specific power of 150 W/kg, representative of the decay heat one hour after SCRAM in a generic PWR. The device is equipped with an outlet steam flowmeter while many thermocouples are located in the heated debris bed and in the bypass zone. In the tests presented hereafter, water is injected at the bottom of the test section (bottom flooding) and the influence of a wide range of parameters is investigated: system pressure from 1 to 5 bars, initial temperature from 400 to 700°C, injection velocity from 2 to 5 m/h, size of particles in the heated debris (2 or 4 mm) and bypass thickness (20 or 45 mm).

The device is modelled in ASTEC by 3 axial channels for the debris bed plus one channel for the bypass, surrounded by an adiabatic wall, and a 50 mm axial nodalization is applied. The bed initial temperature is set to the experimental value measured at the reflooding onset ( $t=0s$ ). A constant pressure boundary condition is applied at the top while water is injected from the bottom following experimental conditions.

Figures 4b and 4c indicate examples of comparison between ASTEC V2.1.1.6 calculation and experiments [33] (very similar results are obtained with ASTEC V2.2). The presented tests D5-2 and D1-7 are both

performed with the same debris bed geometry, water velocity and initial temperature, and only differ by the imposed pressure (respectively 5 bars and 1 bar). The steam mass flow rate at the test section outlet is well reproduced in both tests (oscillations in the ASTEC results are related to the axial nodalization), as well as the quench front evolution in the bed centre ( $R=0$  mm) and periphery ( $R=220$  mm) (due to low temperatures in the bypass, ASTEC criteria for the quench front detection are never fulfilled in this region, so that ASTEC quench front evolution is not presented for  $R=250$ mm on Figure 4c). In particular, the impact of pressure on the reflooding is well captured: while a flat quench front profile is observed in D5-2 test with a short reflooding time, the quench front progression in D1-7 is faster in the periphery compared to the center, and the reflooding time is much longer.

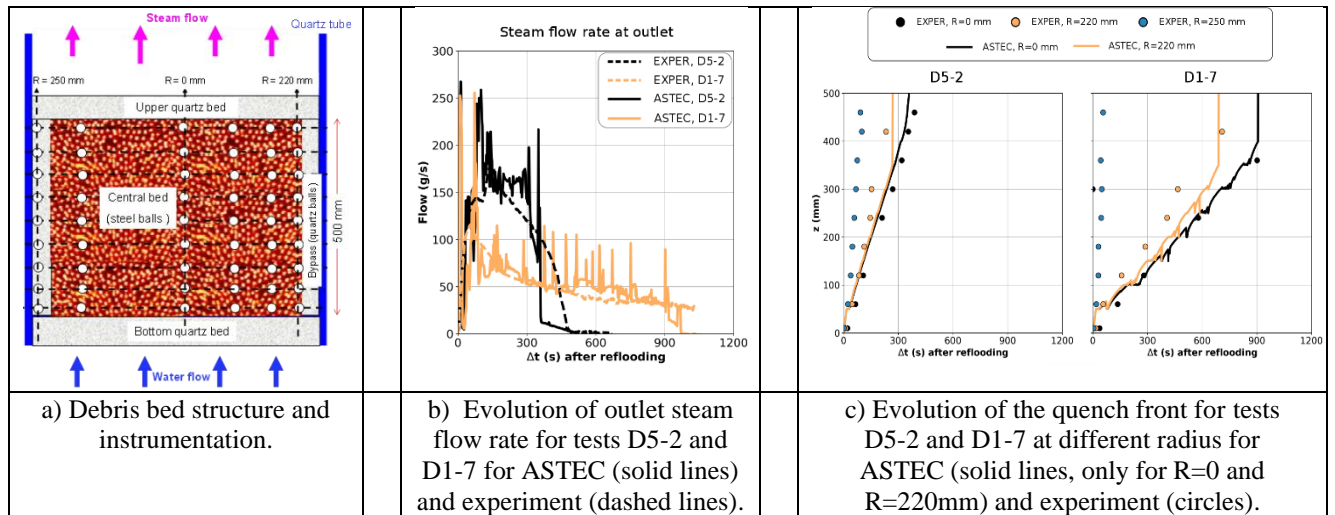


**Figure 4. PEARL:** impact of pressure between tests D5-2 (5 bar, injection at 5m/h, 2mm particles) and D1-7 (1 bar, 5m/h, 2mm).

Furthermore, in close connection with the ASCOM project, RUB PSS completed the validation matrix by analyses of the simulation of several other late phase flooding tests in the German DEBRIS facility [21].

Besides these three illustrative examples, a summary of the main lessons which have been drawn from the whole code-to-data assessment in the field of core degradation is provided later in Section 4. To get more details about these numerous ASTEC V2 CESAR/ICARE simulations, one may refer to [28] [29] [31] [33] [34].

### 3.3. Corium Behavior in the Vessel Lower Head and ERVC issues

As already mentioned, the ICARE module also deals with the corium behavior after its slumping from the core into the lower head. Furthermore, in case of situations with an In-Vessel Retention (IVR) strategy implementation, the CESAR module is also of interest to properly model the external reactor vessel cooling (ERVC) circuit. The validation matrix that was considered to specifically assess both the ICARE and CESAR lower head models is supplied in Table 3. It should be noted that for the modelling of the corium in the vessel lower head and more particularly of the distribution of chemical species in the different corium phases, ASTEC V2.2 relies through correlations [35] on the extensive work, both experimental [36] and modelling, that has been carried out on the thermochemistry of the corium and capitalized in the NUCLEA database [37] developed at IRSN.

**Table 3. Main vessel lower head and ERVC experiments used for ASTEC V2.2 validation**

Domain	Physical phenomena	Facility/ Program	Experiments
Corium-water interaction	Fragmentation of corium in water	FARO	tests #14 (ISP-39) and #24
Corium behavior in lower head	Heat transfer in corium molten pools	LIVE	L1, L6
	Interaction between corium and structural materials	MASCA	21 tests
	Corium oxidation	CORDEB	CD2 series (3 tests)
Vessel mechanical failure	Vessel lower head wall thermal-mechanical loading	OLHF	OLHF-1
IVR / ERVC	Two-phase thermal-hydraulics in external reactor vessel cooling circuit	ULPU-V	M63 series (test #10)
		RESCUE-2	tests #1 and #2
		THS-15	2 test campaigns

RESCUE-2 and THS-15 analyses were carried out by IVS and UJV, respectively, in the frame of the ASCOM project [22] [23].

As an illustration of these works, results from the FARO test #14 simulation obtained with ASTEC V2.2.0 are indicated in Figure 5. In this test, about 100kg of corium (80% of  $UO_2$  in mass fraction, and 20% of  $ZrO_2$ ) are poured in a pool at saturation temperature to study the corium fragmentation and vessel pressurization. Figure 5a shows the mass evolution of the different layers represented in the lower head modelling of ASTEC: the transitory slumping debris (SDEBR), a fragmented debris bed at the bottom (DEBRIS1), three corium layers (only the MAGMA1 corresponding to the oxide layer is significant here), and a debris bed at the top (DEBRIS2). The final mass of debris and corium fits well the experimental values. The vessel pressurization is represented on Figure 5b: the fast pressure rise due to the steam production induced by the corium fragmentation is also well reproduced by ASTEC.

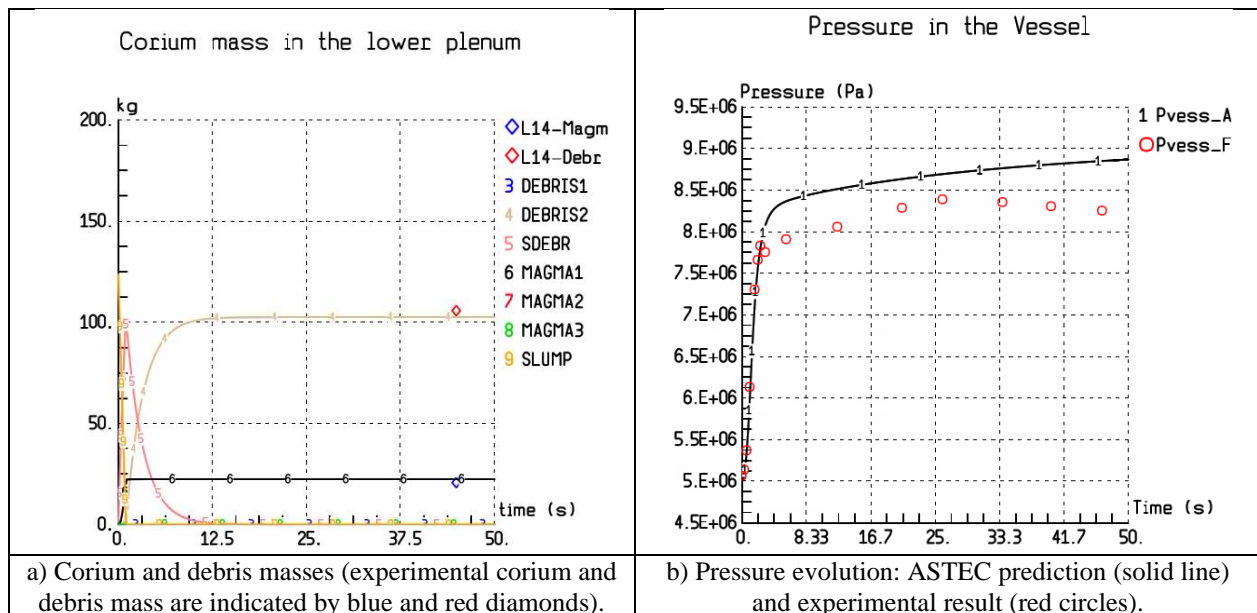
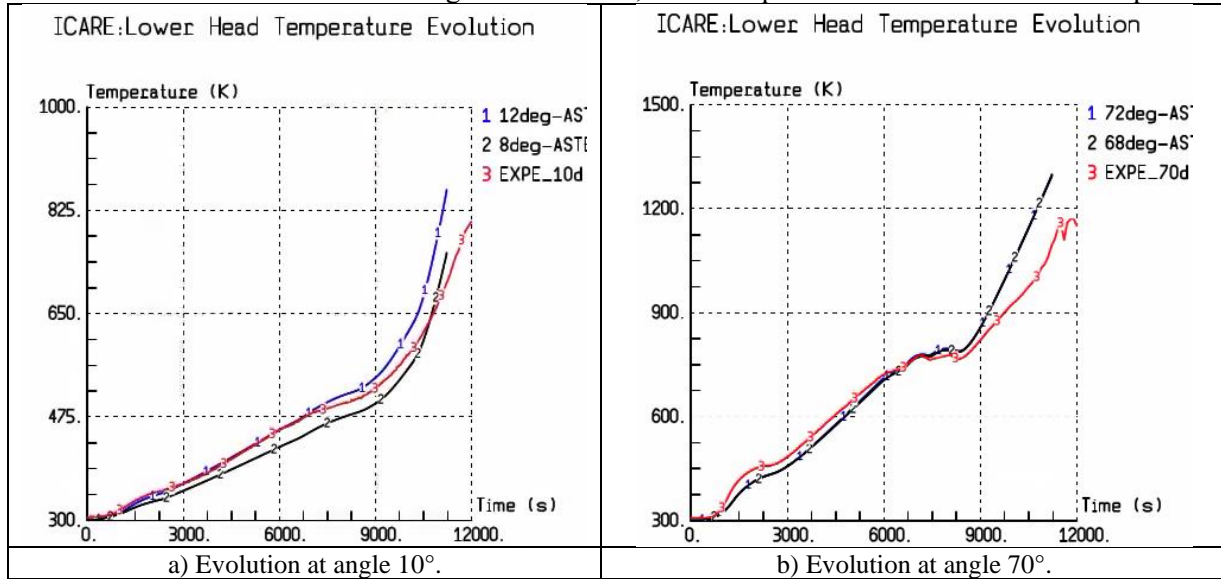


Figure 5. FARO test 14.

As a second illustration of the lower head models validation, Figure 6 indicate the results of ASTEC simulations of the OLHF test 1. In this test, a steel hemispheric lower head is pressurized and heated by induction up to its failure. The evolution of the temperature at the external face of the hemisphere is well

reproduced at the two indicated angles (angle 0° corresponds to the bottom of the hemisphere). ASTEC predicts a failure at 10500 s between angles 63° and 70°, to be compared to 11520 and 75° in the experiment.



**Figure 5. OLHF test 1:** Evolution of the temperature at the external face of the lower head. Experimental results are indicated in red, ASTEC results corresponding to the two neighbouring meshes are indicated in blue and black.

A summary of the main lessons that have been drawn from the code-to-data assessment relating to the corium behavior in the vessel lower head is provided in Section 4. To get more details about these ASTEC V2.2 simulations, one may refer to [28] [29] [38].

### 3.4. Fission Products Release from the Core

In ASTEC, the fission products (FP) release from the core components is simulated by the ELSA module that is tightly coupled with the ICARE module. The validation matrix that was considered to evaluate the physical relevance of the ASTEC V2.2 ELSA FP release models is supplied in Table 4.

**Table 4. Main FP release experiments used for ASTEC V2.2 validation**

Domain	Physical phenomena	Facility/ Program	Experiments
Fission products release	Releases from short fuel rod under steam or H <sub>2</sub> gas (re-irradiated fuel)	VERCORS VERCORS-HT VERCORS-RT	V1, V2, V3, V4, V5 HT1, HT2 RT6
	Releases from high burn-up fuel and MOX fuel, under highly oxidizing atmospheres	VERDON	#1, #2, #3, #4, #5
	Releases from CANDU fuel fragments, under steam or hydrogen carrier gas, low burn-up	MCE HCE	CF2, CM2, LM2, H01, H02, H03, H04, H05, H06
	SIC control rod releases	EMAIC	A, B, C, E

	Release from a 20 fuel rods bundle (early and late degradation phases)	Phébus FP	FPT1 ( <i>ISP-46</i> ), FPT2, FPT3, FPT4
	Release from a particulate debris bed, and then from a molten pool	Phébus FP	FPT4

To illustrate such validation tasks, attention is directed hereafter at the works that have been performed with a preliminary version of V2.2.1 to assess the ELSA module vs. the VERDON 1 and 2 experiments [39] dedicated to FP release from high-burnup fuel under high temperature annealing and in an oxidizing and/or reducing atmosphere, reproducing different SA sequences. The released fraction of different FP representative of the usual classes, namely volatile (Cs), semi-volatile (Mo and Ba) and low-volatile (Ru), are represented on figures 7a and 7b. The overall behavior is well reproduced, especially regarding the dependency of semi and low volatile FP to the oxidizing conditions, although Ba and Ru final release are sometimes overestimated. In VERDON 1, release of Mo occurs during the oxidation plateau by steam and stops with the arrival of reducing  $H_2/H_2O$  atmosphere, while Ba exhibits the opposite behavior. In VERDON 2, the onset of release of Ru under mixed steam-air condition is well captured.

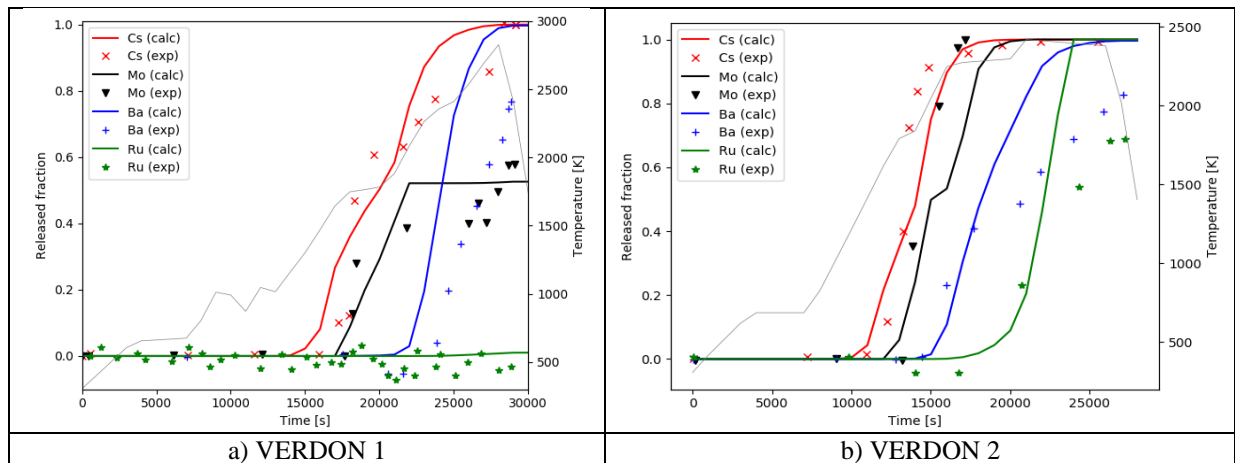


Figure 7. Release of Cs, Mo, Ba and Ru in VERDON tests 1 and 2. Solid lines indicate ASTEC results.

### 3.5. Fission Products and Aerosols Transport and Chemistry in RCS

In ASTEC V2.2, all FP/aerosols phenomena (i.e. transport and chemistry of FPs and aerosols in both the RCS and the containment) are simulated by the SOPHAEROS module. The validation matrix that was considered to evaluate the suitability and capability of the SOPHAEROS models in the RCS domain is supplied in Table 5.

Table 5. Main FP/aerosol transport and chemistry experiments used for ASTEC V2.2 validation

Domain	Physical phenomena	Facility/ Program	Experiments
FP/aerosol behavior in RCS	Diffusiophoresis aerosol deposition	TUBA	TD07
	Interaction between FP vapor and aerosols	FALCON	test #18 ( <i>ISP-34</i> )
	Deposition and resuspension of aerosols	STORM	SR-11 ( <i>ISP-40</i> )
	Iodine transport and chemical speciation in the RCS	CHIP / CHIP+	12 tests

<b>FP/aerosol transport and chemistry in RCS</b>	Cesium transport and interaction with Boron in the RCS	EXSI-AERIS	5 tests
	CsI transport and interaction with Boron and Molybdenum oxides in the RCS	EXSI-PC	5 tests
	Ruthenium transport and chemical speciation in the RCS	START	6 tests
	All FP/aerosols phenomena in RCS	Phébus FP	FPT1 ( <i>ISP-46</i> ), FPT3

To illustrate such validation tasks, attention is directed hereafter at a little part of the works that have been performed with the V2.2b version to assess the SOPHAEROS modeling for iodine gaseous phase chemistry kinetics in the RCS vs. most of the CHIP and CHIP+ experiments. The CHIP experimental program, conducted at IRSN as part of the International Source Term Program (ISTP) [40], aimed to obtain data on iodine speciation under different circuit boundary conditions in presence of other fission products (Cs, Mo) and/or control rod materials (Ag, In, Cd, B) that could be released during the reactor core meltdown. Classically, the CHIP experiments consist in analyzing the behavior of selected elements that are transported in a controlled thermal gradient tube flow. For that purpose, the test line is composed of a high temperature alumina tube at the entrance, followed by a stainless-steel tube where the fluid is cooled down and where the chemical reactions take place, producing aerosols and gases.

Validation results are displayed in Table 6 for two tests (tests “Cd-Mo-Cs-I” and “Ag-Cd-B-Mo-Cs-I”) that were part of the CHIP+ program. For each injected element, the comparison between the ASTEC prediction and the experimental data is focused on the deposited masses in the alumina and steel tubes, respectively, and thus the transported mass flowing out from the test line. In both tests, the SOPHAEROS kinetic modelling implemented in ASTEC V2.2 gives a satisfactory estimation of the iodine total transport (gas+aerosols) along the CHIP+ test line. The transport of cesium and molybdenum is also reasonably predicted, although a bit overestimated, notably for the second test loaded with several control rod materials. On the contrary, the transport of Cadmium (Cd) and Silver (Ag) is largely overestimated by ASTEC, notably in the second test because of a large underestimation of the Cd and Ag deposited masses in the high temperature zone.

**Table 6. Deposition & Transport of Elements along the CHIP Line (in % of element mass injected)**

Experiment and selected elements	Deposited in high temperature zone (alumina tube) (% ii.)		Deposited in transport zone (stainless steel tube) (% ii.)		Released at the outlet of the test line (downstream steel tube) (% ii.)	
	Experiment	ASTEC	Experiment	ASTEC	Experiment	ASTEC
<b>“CdMoCsI”</b>						
<b>Iodine</b>	0.00%	0.00%	13.20%	19.28%	86.80%	80.72%
<b>Cesium</b>	10.00%	1.66%	16.50%	16.06%	73.50%	82.28%
<b>Molybdenum</b>	30.60%	11.18%	10.30%	28.44%	59.10%	60.38%
<b>Cadmium</b>	3.00%	0.00%	41.30%	24.74%	55.70%	75.216%
<b>“AgCdBMoCsI”</b>						
<b>Iodine</b>	0.00%	2.70%	7.20%	11.76%	92.80%	85.53%
<b>Cesium</b>	14.30%	1.47%	10.10%	10.99%	75.60%	87.54%
<b>Molybdenum</b>	25.50%	3.25%	9.10%	10.68%	65.40%	86.06%
<b>Cadmium</b>	33.10%	0.00%	24.20%	18.50%	42.70%	81.50%
<b>Silver</b>	48.50%	17.16%	7.80%	9.01%	43.70%	73.83%
<b>Boron</b>	1.00%	0.03%	1.80%	1.51%	97.20%	98.46%

Overall, the good results obtained for the iodine transport in most CHIP/CHIP+ experiments confirm the physical relevance of the current iodine gaseous phase chemistry kinetics modelling in the RCS. For other elements, results alternate among reasonable (e.g. fuel elements) and inadequate (control rod elements). Modeling challenges therefore remain to be met in this complex field, but improvements are really expected from some IRSN on-going modelling works that aim to ensure SOPHAEROS accounting for non-congruent condensation phenomena.

Furthermore, analyses of the EXSI tests were carried out by VTT [24] as a contribution to the ASCOM project.

A summary of the main lessons that have been drawn from the code-to-data assessment relating to the FP/aerosols behavior in the RCS is provided in Section 4. More information about those ASTEC V2.2 SOPHAEROS analyses are displayed in [28] and [29].

### 3.6. Thermal-Hydraulics in Containment

In ASTEC, CPA is the module dealing with the containment thermal-hydraulics, including all phenomena related to the hydrogen risk (i.e. H<sub>2</sub> distribution, H<sub>2</sub> combustion, H<sub>2</sub> recombination). The validation matrix that was considered at IRSN to evaluate the suitability of the CPA models to address those issues is supplied in Table 7. Results presented below were obtained using ASTEC V2.1.1.6 (same results are obtained with ASTEC V2.2 as the CPA module has not been modified).

**Table 7. Main Containment thermal-hydraulics experiments used for ASTEC validation**

Domain	Physical phenomena	Facility/ Program	Experiments
<b>Thermal-hydraulics in containment</b>	Condensation	TOSQAN	ISP-47
		MISTRA	ISP-47
	Gas mixing, H <sub>2</sub> stratification (with or w/o condensation/evaporation)	THAI	HM-2
		PANDA	T9, T9bis
Sump/gas transfers	TOSQAN	T201	
<b>Performance of mitigation systems</b>	Condensation with spray activation	TOSQAN	T115
		PANDA	PE1
	Hydrogen recombination	THAI	HR-1, HR-11, HR-12 HR-22, HR-23
<b>Gas combustion and flame acceleration in containment</b>	Slow deflagration (H <sub>2</sub> -air-Steam mixture)	THAI	HD-22 ( <i>ISP-49</i> )
	Fast deflagration (H <sub>2</sub> -air-Steam mixture)	ENACCEF	ISP-49, XH2
	Fast deflagration (H <sub>2</sub> -Air mixture)	ENACCEF	run-153

Firstly, to illustrate the validation tasks relating to containment basic thermal-hydraulics, attention is directed hereafter at the work that was performed with the ASTEC V2.1.1.6 revision to assess the CPA module vs. the TOSQAN ISP-47 test. This experiment, operated by IRSN, aimed to study steam condensation on walls, notably in presence of non-condensable gas. For that purpose, the ISP-47 test included three steady states with air-steam mixture and one steady state with air-steam-helium mixture [41].

The global thermal-hydraulics behavior of the TOSQAN ISP47 test is mainly governed by steam injection and wall condensation (pressurization due to steam and helium injection and depressurization due to condensation on cold wall). Each steady state, characterized by a pressure level (Fig. 8a), is reached when

the condensation mass flow rate (Fig. 8b) is equal to the steam injection mass flow rate. As shown on those figures, the ISP-47 thermal-hydraulics behavior is very well captured by the ASTEC V2.1.1.6 CPA simulations for the four steady-states. The fluid temperature evolution is also reasonably predicted during both the pressurization and depressurization phases.

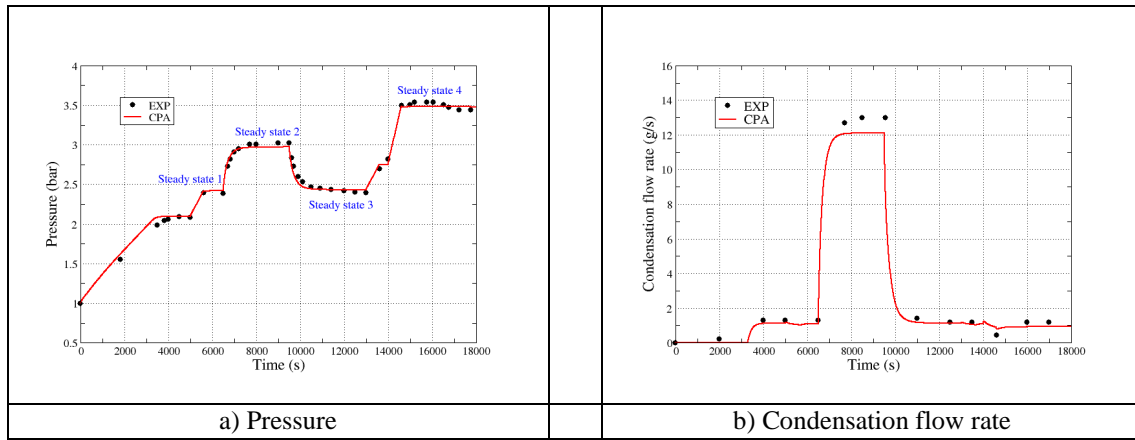


**Figure 8. TOSQAN ISP-47**

Secondly, to illustrate the validation tasks in the field of hydrogen combustion and flame propagation, attention is directed hereafter at the work that was performed with the V2.1.1.6 revision to assess the CPA flame front model vs. the THAI HD-22 test that was part of the ISP-49. This experiment, operated by Becker Technologies GmbH, aimed to study an upward directed deflagration in an air-steam-hydrogen initial atmosphere [42].

Results are displayed for the pressure evolution at elevation 7700 mm and for the flame position along the vessel height centerline. As depicted in Fig. 9a, the timing for the pressure increase does not fit perfectly the experimental measurement (it is a bit anticipated with CPA), but overall the ASTEC V2.1.16 simulation looks quite consistent. The kinetics of pressurization is indeed very well predicted by CPA, as well as the maximum pressure value, and the subsequent slow depressurization kinetics is also well simulated. Besides, the flame propagation along the vessel centerline is also quite well captured by ASTEC (Fig. 9b).

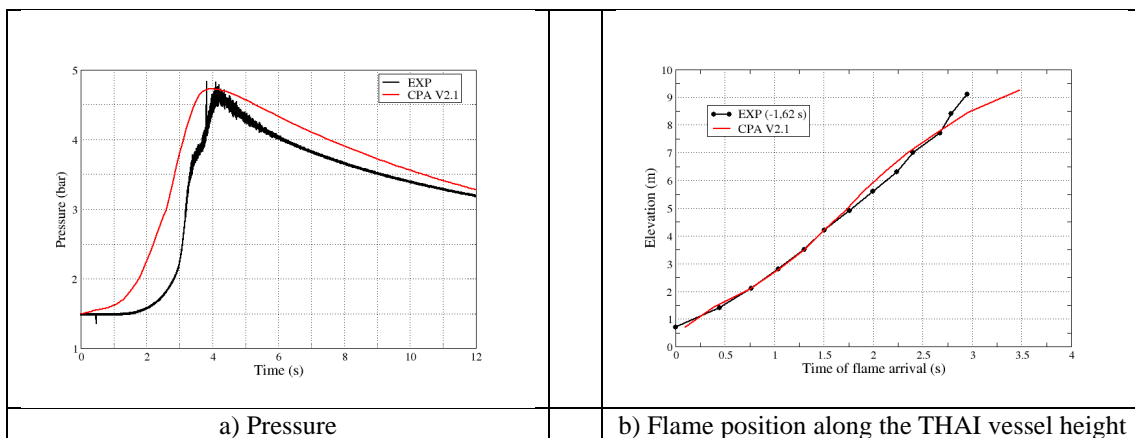


**Figure 9. THAI HD-22**

Thirdly, to illustrate the validation tasks in the field of hydrogen recombination, attention is directed hereafter at the work that was performed with the V2.1.1.6 revision to assess the CPA module vs. the THAI

HR-1 test that aimed to investigate operation behavior of the “Framatome FR-380” passive autocatalytic recombiner (PAR) [42].

Results are displayed for the pressure evolution (Fig. 10a) and the hydrogen concentration evolution at elevation 6600 mm (Fig. 10b). During the PAR operation phase, the CPA predictions match very well the experimental measurements for all selected output parameters (pressure, gas temperature, H<sub>2</sub> recombination rate and H<sub>2</sub> concentration), both on the timing and the magnitude. The recombination rate is in particular quite well evaluated while the pressure peak and the maximum gas temperature are a very little overestimated (0.03 bar and 4°C, respectively) by ASTEC. During the subsequent PAR ignition phase, CPA predictions are still quite satisfactory, despite few minor code-to-data deviations are observed on the pressure and gas temperature peak values (but the time when maximum values are achieved in ASTEC is correct). The same trend is also observed on the H<sub>2</sub> recombination rate (perfect timing for the peak prediction but underestimation of its magnitude), but the discrepancy remains not so large, as confirmed by the proper estimation the H<sub>2</sub> concentration downstream of the PAR.

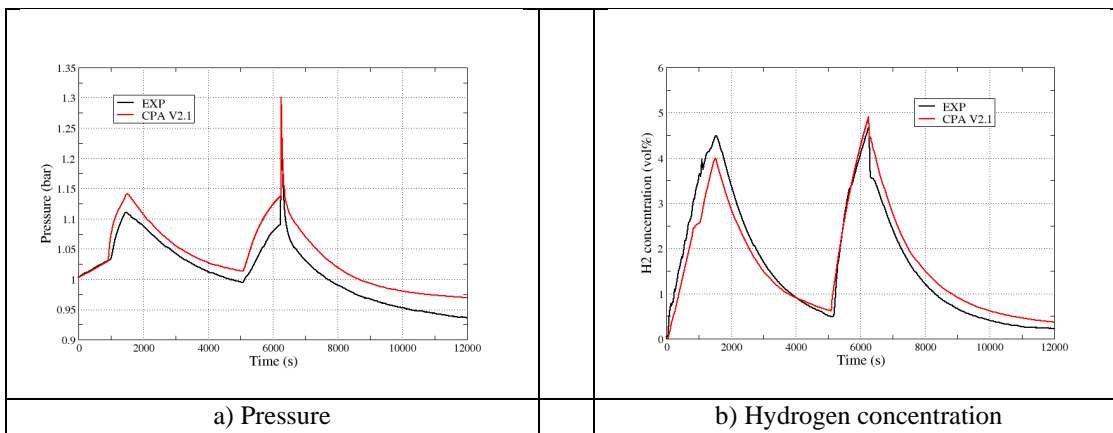


Figure 10. THAI HR-1

A summary of the main lessons that have been drawn from the code-to-data assessment in the field of the containment thermal-hydraulics is provided in Section 4. More details about these numerous and rather different ASTEC V2.1.1.6 CPA analyses may be found in [28] and [29].

### 3.7. Thermal-Hydraulics and Aerosols Behavior in Containment

As already mentioned, the SOPHAEROS module also deals with the behavior of FPs and aerosols in the containment, in addition to its treatment of the RCS domain. The validation matrix that was considered to evaluate the suitability and capability of the SOPHAEROS models to cope with those containment phenomena is supplied in Table 8. The CPA/SOPHAEROS coupling was activated to simulate the integral tests while pool-scrubbing SETs have been calculated using SOPHAEROS in its stand-alone running mode.

Table 8. Main experiments on FP/aerosol behavior in containment used for ASTEC V2.2 validation

Domain	Physical phenomena	Facility/ Program	Experiments
Thermal-hydraulics and aerosols behavior in containment	Thermal-hydraulics and aerosols behavior in containment	VANAM	M3 (ISP-37)
		Phébus FP	FPT1 (ISP-46), FPT3
	Thermal-hydraulics and aerosols behavior in containment with spray	CSE	A10

<b>Filtration</b>	Filtration by pool scrubbing	PSI experim.	5 tests
		VTT experim.	20 tests

Additional analyses were performed by partners in the frame of the ASCOM project, e.g. Tractebel on Phébus FPT3 containment issues [43] and VTT on pool scrubbing tests [44].

To illustrate IRSN validation tasks, attention is directed hereafter at the works that have been performed to assess the CPA/SOPHAEROS coupled modules vs. the ISP-37 VANAM M3 experiment [45] that was conducted at Battelle in the BMC facility representing a simplified multi-compartment containment of a PWR reactor.

As shown for the total pressure evolution (Fig. 11a) and for the aerosols concentration (Fig. 11b), the results of the ASTEC V2.2 calculation are in good enough agreement for both thermal-hydraulics and aerosols behavior in the dome region. However, the stratification of the atmosphere that developed in some other compartments during several phases of the experiment could not be reproduced because of the CPA base nodalization assumptions. As a direct consequence, the aerosol depletion during the last phase is underestimated in the lower zones (Fig. 11c) due to superheated instead of saturated zone conditions.

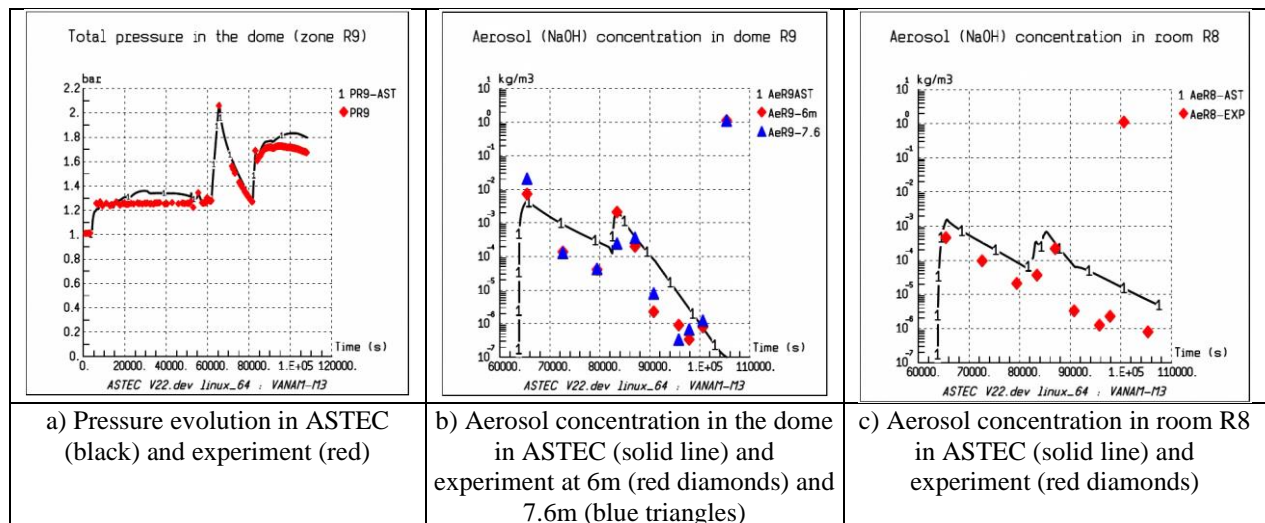


**Figure 11. VANAM M3**

A summary of the main lessons that have been drawn from the code-to-data assessment related to behavior of FPs and aerosols in the containment, along with their coupling to the thermal-hydraulics, is provided in Section 4. To get more details about these ASTEC V2.2 CPA/SOPHAEROS simulations, one may refer to [28] and [29].

### 3.8. Iodine and Ruthenium Chemistry in Containment

In ASTEC V2.2, the SOPHAEROS module also addresses in a detailed manner the chemical behavior of iodine and ruthenium compounds (vapors and aerosols) in the containment. The validation matrix that was considered to evaluate the physical relevance of the SOPHAEROS iodine models in the containment is supplied in Table 9.

**Table 9. Main experiments on containment iodine chemistry used for ASTEC V2.2 validation**

Domain	Physical phenomena	Facility/ Program	Experiments
<b>Iodine chemistry in containment</b>	I <sub>2</sub> formation in sumps and adsorption surfaces	CAIMAN	test 97/02 ( <i>ISP-41</i> )
	Iodine volatility in containment	PHEBUS RTF	RTF1 ( <i>ISP-41</i> ), RFT3, RTF6
	Radiolytic oxidation of I <sup>-</sup> and mass transfers on paints	SREAS	test #01
	Iodine release from Epoxy paints under irradiation	EPICUR LD	LD1, LD2, LD3, LD5, LD6
	Interaction of I <sub>2</sub> with stainless steel	BIP	G1
	CH <sub>3</sub> I desorption from Epoxy paints	BIP2	RAD-EPICUR-A1
	Iodine mass transfer and adsorption on steel walls	THAI	Iod-09
	Silver/Iodine interactions in sumps	Siemens/IPSN	6 tests
	AgI decomposition	STEM2	EPICUR-MCAer1
	IOx formation	PARIS	2 tests
IOx decomposition	STEM2/AER STEM2/IOX	6 tests	
<b>Ruthenium chemistry in containment</b>	Decomposition of RuO <sub>2</sub> on dry paint under irradiation	IRSN	4 tests
<b>Behavior of all FP vapors and aerosols in containment</b>	All iodine and ruthenium chemistry-related phenomena	Phébus FP	FPT1 ( <i>ISP-46</i> ), FPT2, FPT3

To illustrate such validation extended tasks, attention is directed hereafter at the works that have been performed to assess the SOPHAEROS containment iodine chemistry models vs. the PHEBUS RTF1 test and EPICUR-LD6 test, respectively.

The PHEBUS RTF1 test, that had been operated at AECL at the end of the 90s as a part of the ISP-41 [46], dealt notably with the radiolysis of iodide ions I<sup>-</sup> in the sump, leading to the formation of I<sub>2</sub> in the sump and its transfer to the gaseous phase where it was adsorbed on a dry paint surface. So, the main issue of this validation task was to check how fast iodide ions I<sup>-</sup> were converted into gaseous I<sub>2</sub> and how much gaseous organic and inorganic iodine remained in the gaseous phase all over the irradiation. As illustrated below (Fig. 12a, 12b and 12c), the ASTEC V2.2 prediction of the iodine distribution in the aqueous phase, in the gaseous phase and on the painted surfaces was quite good using recommended values for the steel and paint adsorption rate constants.

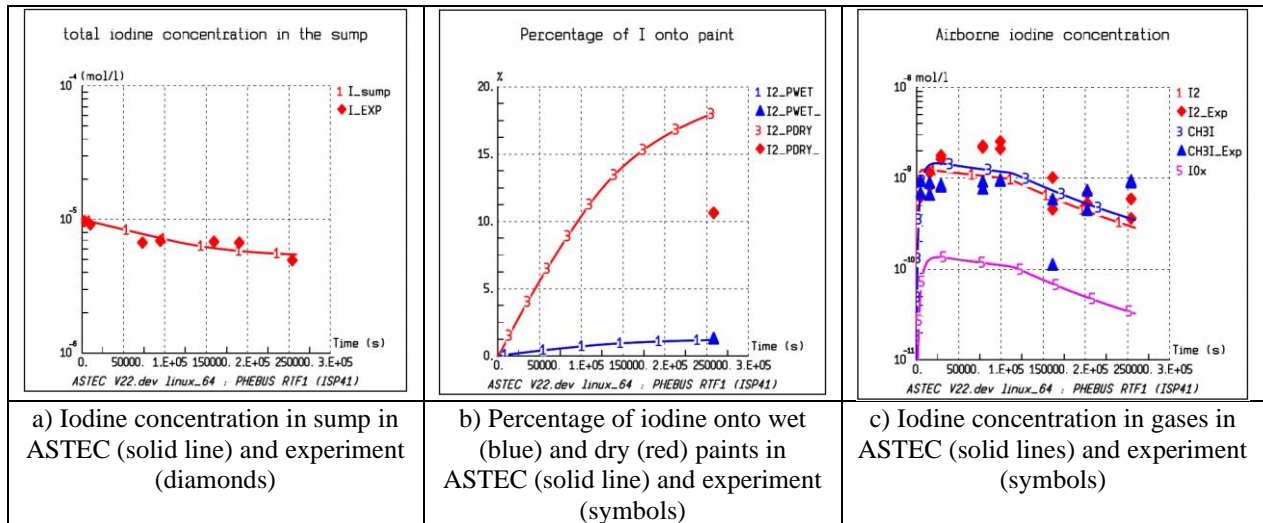


**Figure 12. PHÉBUS RTF1**

The main objectives of the EPICUR LD tests [47] were to quantify the inorganic and organic releases from Epoxy paint loaded with iodine and irradiated in a gaseous environment. For that purpose, the LD series dealt with the irradiation of a painted coupon located in the gaseous phase and a carrier gas was injected to evaluate the kinetics of  $\text{CH}_3\text{I}$  and  $\text{I}_2$  desorption from the coupon under irradiation. So, the main issue of the validation task was to assess the SOPHAEROS new model of iodine-Epoxy paint interaction under irradiation that considers the influence of the temperature, dose rate and iodine concentration on the paint. As illustrated below on Fig. 13a and 13b for the LD6 test, this V2.2 new model allows getting very good results for the release kinetics of both  $\text{I}_2$  and  $\text{CH}_3\text{I}$  species.

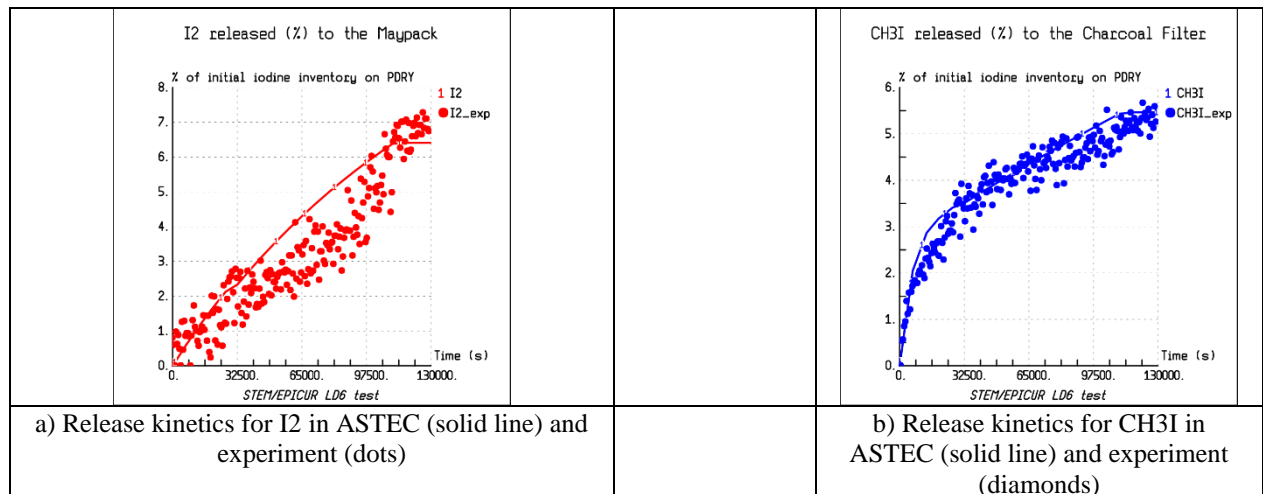


**Figure 13. EPICUR LD6**

A summary of the main lessons that have been drawn from the code-to-data assessment relating to the iodine and ruthenium chemistry in the containment is provided in Section 4. More details about these diverse ASTEC V2.2 SOPHAEROS simulations may be found in [28] and [29].

### 3.9. Direct Containment Heating

In ASTEC the Direct Containment Heating (DCH) is modelled in a rather simple manner, with main goal to limit the number of user parameters that are unknown particularly in reactor cases. The ASTEC V2.2 DCH models were validated on five tests from the KIT DISCO experimental program, focusing on the DISCO-HOT FH series addressing French 1300 MWe PWRs. The main lessons that have been drawn from this assessment are briefly summarized in Section 4. More details may be found in [28] and [29].

### 3.10. Molten Core Concrete Interaction

In ASTEC, MEDICIS is the module dealing with Molten Core Concrete Interaction (MCCI). The validation matrix that was considered to evaluate the suitability of the ASTEC V2.2 MEDICIS models is supplied in Table 10. It must be stressed that, as for the behavior of the corium vessel lower head, having accurate thermochemical data for a corium-concrete mixture is of prime importance for evaluating the temperatures and material transport properties which strongly influence heat transfer distribution within the corium pool. This is achieved through tabulations calculated from the NUCLEA thermodynamic database currently validated at IRSN [37].

**Table 10. Main MCCI experiments used for ASTEC V2.2 validation**

Domain	Physical phenomena	Facility/ Program	Experiments
<b>Corium-Concrete interaction (dry cavity conditions)</b>	Interaction with LCS concrete	OECD-CCI	CCI-2
	Interaction with siliceous concrete	OECD-CCI	CCI-3
		VULCANO	VBU-5, VBU-6
<b>Corium-Concrete interaction with top flooding</b>	LCS concrete	CCI	CCI-8
	Siliceous concrete		CCI-7

To illustrate such validation tasks, attention is directed hereafter at the work that was performed with a preliminary version of V2.2.0 to assess the MEDICIS top quenching models vs. the CCI-8 test. The CCI-8 experiment, conducted at ANL with a fully oxidized 1000 kg PWR core melt [48], aimed to evaluate whether a melted corium interacting with concrete can be cooled down efficiently with early top flooding. Initially, the corium contained 8 wt% of LCS concrete.

Results are displayed below for the axial ablation kinetics (Fig. 14a) and for the cavity shape (Fig. 14c). After an initial burst, the axial erosion appears to progress steadily over the course of the test. This axial ablation kinetic is quite well reproduced by ASTEC V2.2. In contrast, ASTEC/MEDICIS does not predict correctly the delayed start for more than half an hour of the sidewall erosion (Fig. 14b). Moreover, as to the rest of the transient, no definite conclusion can be drawn on the lateral erosion kinetics predicted by ASTEC as the experimental profiles are not symmetrical. Anyhow, it is worth noting that in ASTEC V2.2 a perfect contact between the melt and the crust is always assumed. Without any crust anchoring prediction, MEDICIS predicts a significant ejected corium mass, leading to the formation of a substantial particle bed. The corium is almost entirely erupted, and the calculated layer mass for each layer is not consistent with the experimental observations.

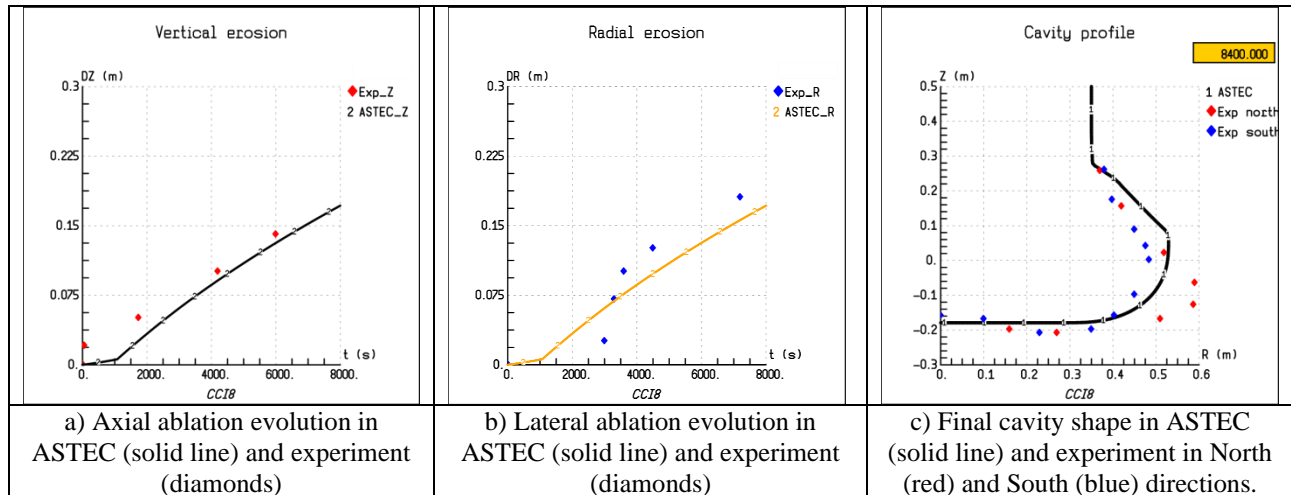


Figure 14. CCI-8

A summary of the main outcomes that have been drawn from the code-to-data assessment in the field of CCI (either dry CCI or CCI with top flooding) is provided in the next section. To get more details about these ASTEC V2.2 MEDICIS analyses, one may refer to [28] and [29].

#### 4. MAIN OUTCOMES FROM ASTEC V2.2 VALIDATION

As concerns the experiments that had been already simulated and analyzed with ASTEC V2 former versions, the V2.2 results were often very close to V2.1, sometimes improved (depending on whether the ASTEC models dealing with the phenomena addressed by the experiments of concern have been updated or not) while we have never experienced any obvious regressions. As expected, the main progress was indeed on the modelling of phenomena that were not (or very poorly) addressed in V2.0 and/or V2.1 and for which new models had been therefore developed since V2.1 (or for which existing models had been largely revised and improved), thus significantly enlarging the validity domain of the ASTEC code.

For primary and secondary circuit thermal-hydraulics, the ASTEC V2.2 models have been successfully reassessed vs. numerous SETs (Moby-Dick, Coturne, Cosi, Patricia...) covering basic key phenomena such as critical flow-rate, flashing, interfacial friction, wall heat transfer, interfacial heat transfer, reflooding of a full-scale western-PWR fuel rod assembly (PERICLES). Good results have been also obtained on several BETHSY integral tests with RCS loops as well as vs. the TMI-2 accident scenario (phases 1 and 2). Besides, satisfactory results had been also previously exhibited on PACTEL experiments using ASTEC V2.1 in the frame of the CESAM project [9], thus illustrating the overall capability of the ASTEC V2 series to properly address RCS thermal-hydraulics for VVER designs.

For core degradation early phase phenomena such as core heat-up, oxidation and hydrogen production, results of the ASTEC V2.2 simulations of several Phébus FP and QUENCH integral experiments are quite good. Furthermore, the core final state is also rather well estimated for all Phébus FP and QUENCH transients. Those results show the overall consistency of the updated early-to-late transition phase modeling now available in V2.2 to trigger the fuel rod embrittlement and subsequent relocation of materials combining the flowdown of solid/liquid melts with the possible formation and collapse of fragmented debris. ASTEC V2.2 results are also satisfactory on TMI-2 up to the final quenching. Conversely, the large hydrogen peaks observed during the late quenching phase are still underestimated by ICARE.

As concerns air ingress transients, the promising results that were obtained few years ago with ASTEC V2.1 against two QUENCH-air rod-bundle integral experiments still need to be updated with V2.2 in order to

adequately assess the relevance of the few recent modelling improvements applied to the ICARE nitriding model.

Furthermore, progressing towards a more adequate modelling of Advanced Tolerant Fuel (ATF) materials represents another challenge to be achieved in the ASTEC future versions. In that respect, IRSN and KIT/INR are jointly participating with ASTEC in the on-going OECD QUENCH-ATF experimental program [49] to acquire new valuable data aimed to support the modelling in that field.

Focusing on late degradation phase models, nice results have been obtained on Phébus FPT4 (test starting in a debris bed geometry), using the combined magma-debris models in the core region. Good results have been also obtained on PRELUDE, PEARL and DEBRIS experiments addressing the reflooding of severely damaged cores, thus confirming the global physical consistency of the ASTEC new model dealing with two-phase flows in porous media. The ICARE modelling for the corium behavior in the lower head was proved to be relevant too, as exhibited by the satisfactory simulations of several LIVE and MASCA tests that were focused on heat transfers in corium molten pools and interaction between corium and structural materials, respectively. Finally, the ASTEC V2.2 lower head failure model was also successfully validated vs. the OLHF-1 experimental data, providing a consistent evaluation of the rupture time and location.

For FP release from core components, good results (and even excellent for volatile species) have been often obtained on both SETs such as VERCORS or VERDON and integral tests such as Phébus FPT1. With respect to previous ASTEC versions, the FP release models have showed a continuous improvement, notably regarding the semi-volatile FP for which a physical model, based on thermo-chemical equilibrium and depending on fuel oxidation and atmosphere composition, has been introduced [50].

Regarding FP/aerosol behavior in the primary circuit, the ASTEC V2.2 results are reasonable on FP transport and deposition, as experienced on TUBA, FALCON and STORM tests. As concerns physical processes that directly drive the amount of iodine to be released under a gaseous form into the containment, suitable results have been also obtained in the field of element chemical speciation in the RCS. In particular, the {Cs-Mo-I-O-H} new models implemented in SOPHAEROS enabled a good prediction of the CHIP PL experimental trends. Those promising results have been then confirmed vs. several tests of the CHIP+ program with control rod materials, apart from the Ag behavior. So, the numerous simulations that have been performed vs. the CHIP and Phébus FP experimental data have clearly highlighted the significant progress that has been brought by the implementation in ASTEC V2.2 of an RCS gaseous phase chemistry kinetics dedicated modelling. Nonetheless, R&D works are still being continued at IRSN on the chemical behavior of multi-element compounds (e.g. on {I-O-H-Cs-Mo-Ag-Cd-B} systems), while progressively ensuring SOPHAEROS accounting for non-congruent condensation phenomena.

For containment thermal-hydraulics, the relevant simulations of TOSQAN, MISTRA, THAI-HM and PANDA experiments confirmed the overall consistency of the ASTEC V2.2 CPA models to deal with mass and heat transfers (e.g. condensation/evaporation, thermal stratification) or hydrogen distribution in the containment under SA conditions. Besides, several other calculations have been performed to specifically assess the modelling relating to some mitigation systems operating in the containment. The simulations of selected TOSQAN and PANDA tests proved the global ability of the CPA models to deal correctly with spray condensation phenomena. The simulations of several experiments from the THAI-HR test series showed that CPA highlight that the behavior of different types of PARs (Framatome-type, AECL-type and NIS-type) is well predicted under various transient conditions. Regarding hydrogen combustion, reasonable results have been also achieved vs. THAI-HD and ENACCEF tests using the specific flame front propagation model. However, open questions still exist applying this model to real plants, as the CPA-FRONT model parameters were determined in relatively small test facilities. So, their application in rougher nodalization with larger control volumes requires to be further assessed.

Regarding the behavior of FPs and aerosols in containment, satisfactory results have been obtained on integral experiments (VANAM, CSE, Phébus FP) using the ASTEC V2.2 SOPHAEROS module. Those rather fair results confirm the physical relevance of the SOPHAEROS containment new modelling that is now replacing the former V2.0 CPA-AFP obsolete sub-module of CPA. This is a valuable outcome for plant complete analyses, as the SOPHAEROS V2.2 extended version allows removing now the discontinuity that has always existed on the treatment of the FP/aerosol species when they moved from the RCS domain to the containment. However, these good results concern mostly the evolution of the species in the gaseous atmosphere or on the walls (suspended and depleted) while the predictions of pool scrubbing experiments still exhibited some modelling deficiencies. The main reason for those latter code-to-data deviations lays likely in a too simplified modelling of the process in the V2.2 version. In that respect, a new pool scrubbing model is being currently under development at IRSN, aimed at removing the observed weakness in that field.

Over the past decade, the ASTEC V2 models dealing with iodine chemistry in containment have been continuously improved in close link with the production of new experimental data successively acquired in the frame of the OECD STEM, STEM2, BIP, BIP2 and BIP3 international projects and the ANR MIRE French domestic project. Most of these SOPHAEROS improvements related to the iodine volatility in gaseous atmosphere aimed at better evaluating the behavior (formation/decomposition) of inorganic and organic iodine species under irradiation. The modelling of iodine aerosols and oxides was also largely improved. All those modelling evolutions (improvements of existing models and development of native models dealing with new processes not addressed in ASTEC former versions) have been then successfully validated vs. numerous SETs. Moreover, in comparison to V2.0 former analyses, a better agreement with experimental data could notably be achieved for all Phébus FP tests on the evolution of both molecular iodine and organic iodine concentrations in the containment. In summary, all these updated validation tasks confirmed that the ASTEC V2.2 SOPHAEROS modelling of the iodine behavior in containment is at the state-of-the-art of the R&D knowledge. Furthermore, though the validation of the SOPHAEROS containment models relating specifically to the behavior of ruthenium species remains much less extended in comparison to iodine, the ASTEC V2.2 modelling of the ruthenium chemistry looked also close to the state-of-the-art, as proved by the quite relevant simulations of IRSN dedicated experiments. That's being said, there are still open issues to be better addressed, such as mid to long term releases. So, modelling efforts in that field shall be continued. In that respect, it is worth mentioning that IRSN actively participates with ASTEC in the on-going OECD ESTER project [51].

Regarding DCH, the ASTEC V2.2 new model, which is less parametric and much simpler than the V2.0 former one, was successfully assessed vs. DISCO FH experiments. In particular, it was shown that, despite its simplifications, this new modelling of the DCH process gave satisfactory results while allowing reducing the number of user parameters which are unknown particularly in reactor cases.

For MCCI in dry conditions, the fair agreement observed between ASTEC V2.2 calculations and experimental data on several CCI and VULCANO experiments for the 2-D ablation kinetics and the final cavity shape, as well as for the ablated concrete mass, shows basically the relevance of the set of assumptions and models used for both considered concrete types (LCS and siliceous). Besides, it is worth reminding here that a good overall agreement with few MOCKA experimental results had been previously exhibited using ASTEC V2.1 in the frame of the CESAM project [9], thus illustrating the capability of ASTEC V2 to also reasonably address MCCI issues in presence of reinforced concrete for the two types of concretes. So, the main still unresolved issue concerning the 2-D ablation in dry conditions remains likely the long-term behavior of the solid accumulation or crust possibly built-up at the cavity bottom very early during MCCI in case of siliceous concrete. For MCCI under water, the CCI-7 and CCI-8 experiments have been selected to make a first assessment of the ASTEC V2 MEDICIS new models specifically addressing the top quenching phenomena occurring during MCCI, such as melt ejection and boiling heat transfers at the corium-water interface, including water ingress. The overall behavior predicted by MEDICIS module

sounded reasonable, although the analyses need to be thoroughly studied. Nonetheless, one must keep in mind that these top quenching models are a priori poorly adapted to the possible anchored crust process and cannot reflect the intermittency of melt ejection. More R&D is therefore still needed on MCCI top quenching regarding these two processes. In that respect, it is worth mentioning that IRSN actively participates with ASTEC in the on-going OECD ROSAU experimental program [52].

Finally, to complement those huge validation tasks carried out vs. experimental data at different scales, a so-called “validation at plant scale” work is also being continuously realized at IRSN. In that respect, the simulation of the TMI-2 real accident transient belongs to the ASTEC V2 large regression testing matrix that is weekly run and checked at IRSN. The analyses of the Fukushima Daiichi accidents are being also periodically updated, notably to further assess the few specific models that aim to better cope with BWR core geometries (e.g. models for the canisters and core sub-channels [3]). Besides, these Fukushima analyses emphasized the need for extending the modelling from the short to the long term in order to better address the delayed releases and resuspension related phenomena [53] [54]. Hence, the ASTEC modelling in those fields will be further improved, accounting for the information that have been already obtained from some OECD recent R&D programs (STEM2 and BIP3) or could come from the on-going OECD ESTER project [51]. Moreover, many other ASTEC V2.2 plant analyses have been performed by foreign partners in the frame of the SNETP-NUGENIA ASCOM project coordinated by IRSN. These independent reactor applications, which often consisted of code-to-code benchmarking calculations, aim at bringing complementary lessons about the overall modelling capabilities of ASTEC V2 to calculate complete SA sequences on diverse types of NPPs (e.g. [15] [16] [55] [56] [57]).

## 5. CONCLUSIONS

The main conclusion that can be drawn from these very extended validation activities of the V2.2 major version is that most ASTEC models are today at the state of the art, in particular FP models that are directly driving the evaluation of the final source term to the environment in case of a severe accident.

ASTEC V2.2 can be considered as a suitable tool to calculate various SA sequences initiated at either reactor power state or shut-down state on different types of NPPs. In particular, as demonstrated by both IRSN and many ASCOM foreign partners, ASTEC V2.2 can be used to perform Gen.II PWR and VVER once-through best-estimate calculations, while providing the actual capability for simulations of technical means for mitigation of SA consequences as well as for simulation of typical SAM actions. For BWRs, the V2.2 containment models and source term models are also considered as physically relevant while the core new degradation models, although proved to be rather consistent, likely need to be further assessed. ASTEC V2.2 can also be used to perform best-estimate safety analyses on EPR, as done at IRSN. Moreover, as demonstrated by several partners, ASTEC V2.2 appears to be also a relevant tool to investigate the progression of severe accidents in NPPs relying on the in-vessel melt retention strategy.

Modelling efforts will continue to keep ASTEC models at the state of the art and thus further improve the simulations of SA relating to various types of Gen.II and Gen.III plants. Besides, both the development of a few new specific models and the improvement of some existing ones are required to enlarge the scope of best-estimate analyses to NPPs equipped with ATF materials in the core as well as to other innovative NPPs and nuclear installations, and in priority to consolidate the promising first ASTEC V2.2 applications to SMRs [58] [59] while better addressing accidents occurring in spent fuel pools [60]. Anyhow, ASTEC shall also remain a repository of knowledge gained from international R&D for SA phenomenology. For that purpose, physical models will be continuously updated according to the interpretation of current and future experimental programs executed in an international frame. Meanwhile, the ASTEC assessment activities will of course continue both at IRSN and outside IRSN through foreign partners’ contributions in the frame of diverse collaborative projects, e.g. MUSA [60], R2CA [61], PASTELS [62], SASPAM-SA [63], etc.

## ACKNOWLEDGMENTS

The authors would like to associate to this article the whole IRSN ASTEC development team who very actively contributed to the ASTEC V2.2 validation tasks, as well as the foreign organizations who also brought afterward a valuable contribution to the ASTEC V2 assessment tasks in the frame of both the international ASTEC Users' Club network and the SNETP-NUGENIA ASCOM project.

## REFERENCES

1. L. Chailan, A. Bentaïb, P. Chatelard, "Overview of ASTEC code and models for Evaluation of Severe Accidents in Water Cooled Reactors", *Proceedings of the IAEA Technical Meeting on Status and Evaluation of Severe Accident Simulation Codes for Water Cooled Reactors*, Vienna (Austria), October 9-12, 2017
2. L. Laborde et al., "Overview of the ASTEC V2.2 integral code", Report IRSN-2021-00298, (2021)
3. P. Chatelard, S. Belon, L. Bosland, L. Carénini, O. Coindreau, F. Cousin, C. Marchetto, H. Nowack, L. Piar, L. Chailan, "Main modelling features of ASTEC V2.1 major version", *Annals of Nuclear Energy*, **93**, pp.83-93, (2016)
4. J.-A. Zambaux, L. Laborde, P. Ruyer, "Calculating steam-water flows at large non-condensable gas concentration with severe accident code ASTEC V2.2", *Proceedings of the 19<sup>th</sup> International Topical Meeting on Nuclear Reactor Thermal Hydraulics (NURETH-19)*, Brussels, Belgium, March 6-11, 2022
5. J.-A. Zambaux, L. Laborde, "Interfacial heat transfer with non-condensable gas in ASTEC V2.2: Application to severe accidents study during PWR cold shutdown states", *Nuclear Engineering and Design*, **411**, 112434, (2023)
6. L. Carénini, F. Fichot, "Evaluation of the kinetics of molten pool stratification in case of In-Vessel Melt Retention strategy", *26<sup>th</sup> International Conference on Nuclear Engineering (ICONE-26)*, London (Great Britain), July 22-26, 2018
7. SNETP NUGENIA TA2 ASCOM, <https://snetp.eu/project-portfolio/>, (2018)
8. P. Chatelard, S. Arndt, B. Atanasova, G. Bandini, A. Bleyer, T. Brähler, M. Buck, I. Kljenak, B. Kujal, "Overview of the ASTEC V2.0rev1 validation", *Nuclear Engineering and Design*, **272**, pp.136-151, (2014)
9. H. Nowack, P. Chatelard, L. Chailan, S. Hermsmeyer, V.H. Sanchez-Espinoza, L.E. Herranz, "CESAM - Code for European Severe Accident Management, EURATOM project on ASTEC improvement", *Annals of Nuclear Energy*, **116**, pp.128-136, (2018)
10. M. Buck, C. D'Alessandro, H. Nowack, P. Chatelard, L. Laborde, L. Carénini, A. Commandé, L. Bosland, I. Gómez García-Toraño, R. Iglesias, J. Fontanet, G. Bandini, S. Ederli, M. Bachraty, P. Matejovic, P. Kostka, G. Lajtha, F. Gremme, A. Stefanova, I. Kljenak, M. Sangiorgi, A. Nieminen, "Synthesis of validation of ASTEC V2.1rev0 and rev1 versions", CESAM FP7 Deliverable referred to as "CESAM-D20.25", (2017)
11. P. Chatelard, N. Reinke, A. Ezzidi, V. Lombard, M. Barnak, G. Lajtha, J. Slaby, M. Constantin, P. Majumdar, "Synthesis of the ASTEC integral code activities in SARNET. Focus on ASTEC V2 plant applications", *Annals of Nuclear Energy*, **74**, pp.224-242, (2014)
12. C. Lombardo et al, "Synthesis of evaluation of the impact of SAM actions through ASTEC NPP calculations", CESAM FP7 Deliverable referred to as "CESAM-D40.44", (2017)
13. N. Andrews, S. Belon, C. Bouillet, H. Bonneville, C. Faucett, "MELCOR-ASTEC crosswalk of the Accident at Fukushima-Daiichi Unit 1 – Phase I Analysis", *International Agreement Report NUREG/IA-0510*, published by U.S. Nuclear Regulatory Commission, (2019)
14. J. Duspiva, M. Kotouč, P. Matejovic, M. Barnak, I. Melnikov, "Benchmark analysis of LB LOCA with reactor cavity flooding for VVER-1000/V320 NPP", *Proceedings of the 9<sup>th</sup> European Review Meeting on Severe Accident Research (ERMSAR-2019)*, Prague (Czech Republic), March 18-20, 2019
15. G. Agnello, S. Ederli, P. Maccari, F. Mascari, "Analysis of an unmitigated 2-inch cold leg LOCA transient with ASTEC and MELCOR codes", *Journal of Physics, Conference Series*, *in press* (2022)

16. M. Di Giuli, M. Malicki, P. Dejardin, V. Corda, A.M. Swaidan, "MELCOR 2.2-ASTEC V2.2 crosswalk study reproducing SBLOCA and CSBO scenarios in a PWR1000-like reactor - part I: Analysis of RCS thermal-hydraulics and in-vessel phenomena", *Nuclear Engineering and Design*, **in press**, (2021)
17. A.K. Mercan, V.H. Sanchez-Espinoza, F. Gabrielli, "Validation of ASTEC 2.1 using QUENCH-12 for VVER reactors", *Proceedings of the 9<sup>th</sup> European Review Meeting on Severe Accident Research (ERMSAR-2019)*, Prague, Czech Republic, March 18-20, 2019
18. O. Murat, V.H. Sanchez-Espinoza, S. Wang, J. Stuckert, "Preliminary validation of ASTEC V2.2 with the QUENCH-20 BWR bundle experiment", *Nuclear Engineering and Design*, **370**, (2020)
19. A. Stakhanova, F. Gabrielli, V.H. Sanchez-Espinoza, A. Hoefer, E. Pauli., "Uncertainty and Sensitivity Analysis of the QUENCH-08 experiment using the FSTC tool", *Annals of Nuclear Energy*, **169(2)** (2022)
20. P. Maccari, S. Ederli, M. Massone, A. Bersano, F. Gabrielli, F. Mascari, "QUENCH-06 uncertainty exercise - ENEA results using ASTEC-RAVEN coupling for uncertainty analysis", *Proceedings of the IAEA Consultancy meeting on QUENCH-06 exercise based on the CRPI31033 findings*, Virtual Event, January 26, 2021
21. J.M. Peschel, C. Bratfisch, M.K. Koch, "Analysis of the reflooding process in degraded particle beds by simulations of the DEBRIS test facility with the severe accident analysis code ASTEC V2.1 and COCOMO code", *Proceedings of the 28<sup>th</sup> International Conference on Nuclear Engineering (ICONE-28)*, Virtual Event, August 4-6, 2021
22. M. Bachraty, "IVS contribution to the NUGENIA-TA2 ASCOM project's third year", ASCOM-WP3 report referred to as "SARNET-ASCOM-VALIDA-R31", (2021)
23. M. Kotouč, "Simulation of external reactor vessel cooling with the ASTEC code – Validation on experiments performed at the THS-15 (VVER-1000) facility", *Proceedings of the 19<sup>th</sup> International Topical Meeting on Nuclear Reactor Thermal Hydraulics (NURETH-19)*, Brussels, Belgium, March 6-11, 2022
24. M. Gouëllou, J. Hokkinen, E. Suzuki, N. Horiguchi, M. Barrachin, F. Cousin, "Interaction between Cesium Iodide Particles and Gaseous Boric Acid in a Flowing System through a Thermal Gradient Tube (1030 K to 450 K) and Analysis with ASTEC/SOPHAEROS", *Progress in Nuclear Energy*, **138**, (2021)
25. N. Trégourès, G. Bandini, L. Foucher, J. Fleurot, P. Meloni, "Validation of CESAR thermal-hydraulics module of ASTEC V1.2 code on BETHSY experiments", *Journal of Power and Energy Systems*, **2**, pp.386-396, (2008)
26. I. Gomez-Garcia-Torano, L. Laborde, "Validation of selected CESAR friction models of the ASTECV21 code based on Moby Dick experiments", *Journal of Nuclear Engineering and Radiation Science*, **5**, (2019)
27. I. Gomez-Garcia-Torano, L. Laborde, J.A. Zambaux, "Overview of the CESAR thermalhydraulics module of ASTEC V2.1 and selected validation studies", *Proceedings of the International Youth Nuclear Congress (IYNC2018) - 26<sup>th</sup> WiN Global Annual Conference*, Bariloche, Argentina, March 11-17, 2018
28. P. Chatelard, "ASTEC V2.1 final validation report", Report IRSN-2019-00717, (2019)
29. L. Laborde et al., "ASTEC V2.2 physical validation", Report IRSN-2021-00272, (2021)
30. D. Jacquemain, S. Bourdon, A. de Bremaecker, M. Barrachin, "Phébus FPT1 : Final Report", Report IPSN/DRS/SEA/PEPF 2004-06, PHEBUS FP/IP 00-479, (2000)
31. O. Coindreau, L. Laborde, F. Fichot, "Validation of ASTEC V2.1 on Q03, Q11 and Q17 experiments", *Proceedings of the 20<sup>th</sup> International QUENCH Workshop*, Karlsruhe, Germany, November 2014
32. **PROGRES** program, <https://www.irsn.fr/EN/Research/Research-organisation/Research-programmes>
33. I. Gomez-Garcia-Torano, L. Laborde, F. Fichot, H. Mutelle, "Reflooding of degraded cores in ASTEC V2.1: modelling and validation on PEARL experiments", *Nuclear Engineering and Design*, **393**, 111768, (2022)
34. I. Gomez-Garcia-Torano and L. Laborde, "Modelling reflooding of intact core geometries in ASTEC V2.1: Improvements and validation on PERICLES experiments", *Nuclear Engineering and Design*, **378**, 111157, (2021)

35. S. Nandan, F. Fichot, B. Piar, A simplified model for the quaternary U-Zr-Fe-O system in the miscibility gap, *Nuclear Engineering and Design*, **364**, 160608, (2020)
36. M. Barrachin, “Corium Experimental Thermodynamics: A Review and Some Perspectives”, *Thermo 1* p 179-204, (2021)
37. E. Fischer, “NUCLEA Thermodynamic Database for Corium, and Mephista Thermodynamic Database for Fuel Applications”, Institut de Radioprotection et Sûreté Nucléaire, St Paul lez Durance, France, 2021
38. L. Laborde, L. Carénini, F. Fichot, “External Reactor Vessel Cooling modelling in ASTEC V2.1 code”, *Proceedings of the 12<sup>th</sup> International Topical Meeting on Nuclear Thermal-Hydraulics, Operation and Safety (NUTHOS-12)*, Qingdao, China, October 14-18, 2018
39. Y. Pontillon, E. Geiger, C. Le Gall, S. Bernard, A. Gallais-During, P.P. Malgouyres, E. Hanus, G. Ducros, “Fission products and nuclear fuel behaviour under severe accident conditions part 1: Main lessons learnt from the first VERDON test”, *Journal of Nuclear Materials*, Volume 495, 2017, Pages 363-384, ISSN 0022-3115, <https://doi.org/10.1016/j.jnucmat.2017.08.021>.
40. **ISTP** program, <https://www.irsn.fr/EN/Research/Research-organisation/Research-programmes>
41. J. Malet, E. Porcheron, J. Vendel, “OECD International Standard Problem ISP-47 on containment thermal-hydraulics: Conclusions of the TOSQAN part”, *Nuclear Engineering and Design*, **240**, pp. 3209-3220, (2010)
42. S. Gupta, E. Schmidt, B. von Laufenberg, M. Freitag, G. Possa, F. Funke, G. Weber, “THAI test facility for experimental research on hydrogen and fission product behaviour in light water reactor containments”, *Nuclear Engineering and Design*, **294**, p 183-201, (2015)
43. M. di Giuli, “Contribution of Tractebel to the NUGENIA-TA2 ASCOM project’s second year”, ASCOM-WP3 report referred to as “SARNET-ASCOM-VALIDA-R23”, (2021)
44. A. Korpinen, “Contribution of VTT to the NUGENIA-TA2 ASCOM project’s second year”, ASCOM-WP3 report referred to as “SARNET-ASCOM-VALIDA-R25b”, (2021)
45. M. Firmhaber, T. Kanzleiter, S. Schwarz, G. Weber, “International Standard Problem (ISP) n°37, VANAM M3 - A multi-compartment aerosol depletion test with hygroscopic aerosol material. Comparison report”, OECD/NEA/CSNI/R(96)26, (1996)
46. J. Ball et al., “International Standard Problem n°41, Containment Iodine Computer Code Exercise Based on a Radioiodine Test Facility (RTF) experiment”, OECD/NEA/CSNI/R(2000)6, Vol 2, (2000)
47. L. Bosland, J. Colombani, “Study of iodine releases from epoxy and polyurethane paints under irradiation and development of a new model of iodine-Epoxy paint interactions for PHÉBUS and PWR severe accident”, *Journal of Radioanalytical and Nuclear Chemistry*, **314**, Issue 2, p 1121-1140, (Nov.2017)
48. M. T. Farmer, B. Tourniaire, K. Atkhen, “Molten Core Concrete Interaction with Early Top Flooding: Results of the CCI-8 Experiment”, *Proceedings of 17<sup>th</sup> International Topical Meeting on Nuclear Reactor Thermal Hydraulics (NURETH-17)*, Xi’an, China, 2017
49. T. Hollands, L. Lovasz, F. Gabrielli, L. Carénini, D. Luxat, J. Phillips, “Status of modeling of FeCrAl claddings in severe accident codes and application on the QUENCH-19 experiment”, *Proceedings of the 10<sup>th</sup> European Review Meeting on Severe Accident Research (ERMSAR-2022)*, Karlsruhe, Germany, May 16-19, 2022
50. G. Brillant, C. Marchetto, W. Plumecocq, “Fission product release from nuclear fuel I. Physical modelling in the ASTEC code”, *Annals of Nuclear Energy*, **61**, p 88-95, (2013)
51. OECD/NEA **ESTER** project (Experiments on Source Term for Delayed Releases), [2020-2024]
52. OECD/NEA **ROSAU** project (Reduction Of Severe Accidents Uncertainties), [2019-2024]
53. C. Bouillet, H. Bonneville, F. Cousin, OECD/NEA BSAF project (Benchmark on the Study of the Accident at the Fukushima Daiichi NPPs), IRSN contribution to BSAF Phase II, Report IRSN/PSN-RES/SAG/2018-00065, (2018)
54. P. Chatelard, F. Gabrielli, F. Fichot, H. Bonneville, C. Bouillet, S. Belon, V.H. Sanchez Espinoza, L. Chailan, “Contribution of ASTEC numerical simulations to the understanding of the Fukushima

- accidents”, *Proceedings of the IAEA Workshop on advances in understanding the progression of severe accidents in Boiling Water Reactors*, Vienna, Austria, July 17-21, 2017
55. M di Giuli, P. Dejardin, M. Auglaire, “Assessment of long-term containment conditions using MELCOR 2.2 and ASTEC V2.2 codes”, *RCCS-2021-OECD/NEA Specialist Workshop on Reactor core and containment cooling systems – long term management and reliability*, Virtual Event, October 18-21, 2021
  56. A. Stakhanova, F. Gabrielli, V.H. Sanchez-Espinoza, E. Pauli, A. Hofer, “Preliminary Uncertainty and Sensitivity Analysis of the ASTEC simulations results of a MBLOCA scenario at a Generic KONVOI Plant using FSTC tool”, *Proceedings of the 10<sup>th</sup> European Review Meeting on Severe Accident Research (ERMSAR-2022)*, Karlsruhe, Germany, May 16-19, 2022
  57. P. Matejovic, M. Barnak, M. Bachraty, L. Vranka, Z. Tuma, “VVER-440/V213 long-term containment pressurization during”, *Nuclear Engineering and Design*, **377**, (2021)
  58. P. Maccari, J.-A. Zambaux, A. Bersano, “BEPU analysis of a 2-inches DVI line break in a generic IRIS SMR by ASTEC-RAVEN coupling”, *EUROSAFE Forum 2021*, Paris, France, November 22-23, 2021
  59. P. Maccari, F. Mascari, S. Ederli, “Analysis of BDBA sequences in a generic IRIS reactor using ASTEC code”, *Proceedings of the 10<sup>th</sup> European Review Meeting on Severe Accident Research (ERMSAR-2022)*, Karlsruhe, Germany, May 16-19, 2022
  60. O. Coindreau, L.E. Herranz, R. Bocanegra, S. Ederli, P. Maccari, O. Cherednichenko, A. Iskra, P. Groudev, P. Vryashkova, P. Petrova, A. Kaliatka, V. Vileiniškis, M. Malicki, T. Lind, O. Kotsuba, I. Ivanov, F. Giannetti, M. D’Onorio, P. Ou, L. Feiye, M. Salay, P. Piluso, Y. Pontillon, M. Nudi, “Uncertainty quantification for a severe accident sequence in a SFP in the frame of the H-2020 Project **MUSA**: first outcomes”, *Proceedings of the 10<sup>th</sup> European Review Meeting on Severe Accident Research (ERMSAR-2022)*, Karlsruhe, Germany, May 16-19, 2022
  61. N. Girault, T. Kaliatka, M. Salmaoui, F. Mascari, N. Muellner, A. Berzhnyi, M. Cherubini, A. Malkhasyan, P. Van-Uffelen, A. Arkoma, Z. Hózer, M. Jobst, L. Luzzi, A. Kecek, D. Gumenyuk, E. Poullier, L.E. Herranz, P. Bradt, V. Busser, “**R2CA** project for evaluation of radiological consequences at design basis accidents and design extension conditions for LWRs: motivation and first results”, *Proceedings of the 10<sup>th</sup> European Review Meeting on Severe Accident Research (ERMSAR-2022)*, Karlsruhe, Germany, May 16-19, 2022
  62. V. Tulkki and M. Montout, “Ensuring safety with passive systems - ELSMOR and PASTELS projects”, *10<sup>th</sup> edition of the Euratom research and training conferences on fission safety of reactor systems (FISA-2022)*, Lyon, France, May 30 - June 3, 2022
  63. HORIZON-EURATOM-2021-NRT-01 - Project: 101059853 - **SASPAM-SA** (Safety Analysis of SMR with Passive Mitigation Strategy - Severe Accident), [2022-2026]